Study of the acidic character of modified metal oxide surfaces using the test of isopropanol decomposition

A. Gervasini

Dipartimento di Chimica Fisica ed Elettrochimica, Università degli Studi di Milano, Via Golgi 19, 20133 Milan, Italy

J. Fenyvesi and A. Auroux *

Institut de Recherches sur la Catalyse, CNRS, 2 Av. A. Einstein, 69626 Villeurbanne Cedex, France
E-mail: auroux@catalyse.univ-lyon1.fr

Received 16 May 1996; accepted 20 November 1996

The evolution of the acid/base properties of a series of oxide supports (alumina, magnesia and silica) modified by increasing loadings of additive ions (Li^+, Ni^{2+}, and SO_4^{2-}) from 1 to 50% of the support surface coverage is reported using the catalytic test of isopropanol decomposition, studied as a function of the reaction temperature. The calculated kinetic parameters E_a, A, and $\Delta S^{\neq}$ permit interpretation of the reaction mechanism with relation to the acidity/basicity of the modified surfaces. The series of alumina oxides, due to the amphoteric properties of the surfaces, decomposed isopropanol through an E_2 mechanism leading to propene and di-isopropyl ether formation. The selectivity to the two products was dependent on the strength of the basicity (addition of lithium and nickel) or on the acidity (addition of sulfate) of the surfaces. Magnesia series oxides dehydrated isopropanol through an E_{1b} mechanism due to the presence of very strong basic surfaces possessing some weak acid sites. The very weak amphoteric character of silica was strengthened by the loading of the three additives; the modified silica surfaces displayed enhanced decomposition activity with respect to pure silica.

Keywords: metal oxides, acidity, isopropanol decomposition

1. Introduction

Supported metal oxide catalysts have obtained much attention because of their wide application as oxidation catalysts and/or as precursors to supported metal and sulfide catalysts. Studies on the nature of the interaction between the dispersed metal oxide species and the support have shown that their catalytic behavior and their acid–base properties are strongly affected by the inductive effect of the metal ions in the solids [1,2].

In previous papers [3,4] have been reported the results of the microcalorimetric and catalytic studies of the acidic character of pure oxide supports (alumina, magnesia, and silica) and the relevant doped oxides by the addition of very small amounts of metal ions (Ca^{2+}, Li^+, Nd^{3+}, Ni^{2+}, SO_4^{2-}, Zr^{4+}) in a concentration of 0.1–0.3 μmol/m^2 which corresponds to a surface coverage of the oxide support of about 0.5–1% of mol of metal ion per mol of support. The aim of the present study has been to extend our investigation to supported oxide samples by varying the amount of the additive on the oxide support (from 3 up to 50% in ion surface coverage of the support). In this approach we have considered both the nature of the guest metal oxide and the surface structure of the host support, which include:

(a) Three different supports, such as an amphoteric γ-alumina, a weakly acidic silica and a basic magnesia. These supports provide different capacities for the formation of highly dispersed species for many metal oxides and induce metal oxide–support interactions of various strengths.

(b) Three different guest metal ions such as lithium, nickel and sulfate ions which exhibit various acid–base properties especially at low loadings.

(c) Three estimated values of metal oxide loadings estimated as 1, 10 and 50% of the monolayer capacity of the supports. In fact, the corresponding experimental values were not always close to the calculated values, mainly on silica which involves different types of oxide phase interactions. However, the sample loadings will be referred to as 1, 10 or 50 for simplification.

In spite of numerous works [5–8] no general correlation between acid–base properties and the amounts of added oxide has been formulated. In particular, how the acidity changes, for a particular ion, the loading varies from a very low amount, creating an ion-doping effect, to an added oxide content up to a monolayer coverage.

The decomposition of isopropanol has been applied to these systems as a method of characterizing the phase composition and the mode of dispersion of the active phase on the support: it provides a quick test for evaluation of catalysts, and for checking the adequacy of a preparation method in producing the optimal acidic cat-

* To whom correspondence should be addressed.

alyst [3,6]. The results are compared with the acid–base properties of the same samples determined previously [9] by adsorption microcalorimetry of various probe molecules.

2. Experimental

2.1. Preparation of the doped and supported oxides

The three host supports, γ-Al_2O_3 (from Akzo-Chemie), MgO (from Carlo Erba), and SiO_2 (from Grace Catalysts & Carriers) were the same oxides as those used in the previous works [3,4]. Besides the doped oxides with Li^+, Ni^{2+}, and SO_4^{2-} additives on γ-Al_2O_3 (referenced as Li(Ni,S)-Al-1), on MgO (referenced as Li(Ni,S)-Mg-1), and on SiO_2 (referenced as Li(Ni,S)-Si-1) prepared as reported in ref. [3], three new series of samples with different amounts of guest oxides have been prepared. They are referenced as Li(Ni,S)-Al(Mg,Si)-10 or as Li(Ni,S)-Al(Mg,Si)-50 depending on the amount of guest oxide on the support expressed as percent of mol of metal ion per mol of support. The composition of the loaded oxides ranged in the interval 3–10% for Li(Ni,S)-Al(Mg,Si)-10 and 15–50% for Li(Ni,S)-Al(Mg,Si)-50. Table 1 collects the samples, their quali–quantitative composition, expressed in ionic concentration and percentage of surface coverage of the guest ions [3,10] as calculated from the surface area values and the chemical analyses of the samples.

The doped and the supported oxides were prepared by incipient wetness impregnation of weighed amounts of the host oxides in powder form (impregnation point of Al_2O_3, MgO and SiO_2 of 1, 4, and 3 ml/g, respec-

Table 1
Physico-chemical properties of the loaded oxides

Sample	Composition M (wt%)	Ionic concentration [a] (μmol/m^2)	Surface coverage [b] (% mol ion/mol support)	Surface area (m^2/g)	Adsorbed volume [c] (μmol/g)	
					NH_3	SO_2
Al	Al_2O_3 (100)	–	–	208	497	470
Li-Al-1	Li(0.015)–Al_2O_3	0.10	0.50	210	544	492
Li-Al-10	Li(0.22)–Al_2O_3	1.49	7.12	212	639	563
Li-Al-50	Li(1.75)–Al_2O_3	13.25	56.7	190	625	713
Ni-Al-1	Ni(0.135)–Al_2O_3	0.11	0.52	203	558	486
Ni-Al-10	Ni(2.43)–Al_2O_3	2.05	9.31	202	585	539
Ni-Al-50	Ni(10.0)–Al_2O_3	9.46	38.3	180	670	55
S-Al-1	S(0.115)–Al_2O_3	0.18	0.80	201	505	498
S-Al-10	S(0.60)–Al_2O_3	0.85	4.2	219	611	318
S-Al-50	S(2.94)–Al_2O_3	3.67	20.6	250	639	88
Mg	MgO (100)	–	–	110	102	407
Li-Mg-1	Li(0.007)–MgO	0.08	0.23	125	201	618
Li-Mg-10	Li(0.08)–MgO	7.19	2.78	16	187	77
Li-Mg-50	Li(0.85)–MgO	87.36	29.5	14	–	135
Ni-Mg-1	Ni(0.10)–MgO	0.15	0.41	112	158	803
Ni-Mg-10	Ni(0.80)–MgO	1.05	3.3	129	320	657
Ni-Mg-50	Ni(3.45)–MgO	4.94	14.2	119	252	651
S-Mg-1	S(0.10)–MgO	0.26	0.76	119	151	686
S-Mg-10	S(0.15)–MgO	0.33	1.12	139	313	763
S-Mg-50	S(1.36)–MgO	2.49	10.23	170	434	692
Si	SiO_2 (100)	–	–	310	91	8
Li-Si-1	Li(0.020)–SiO_2	0.10	0.46	280	144	16
Li-Si-10	Li(0.34)–SiO_2	1.75	7.84	279	361	87
Li-Si-50	Li(2.79)–SiO_2	16.12	64.4	249	289	139
Ni-Si-1	Ni(0.26)–SiO_2	0.14	0.70	307	120	10
Ni-Si-10	Ni(3.67)–SiO_2	2.22	10.0	281	172	38
Ni-Si-50	Ni(17.3)–SiO_2	8.80	47.2	335	342	175
S-Si-1	S(0.072)–SiO_2	0.08	0.36	276	124	10
S-Si-10	S(0.15)–SiO_2	0.17	0.63	281	97	–

[a] Concentration of the metal ion deposited on pure Al_2O_3, MgO and SiO_2 oxides.
[b] Surface ion coverage with respect to pure Al_2O_3, MgO and SiO_2 expressed in metal ion mol to oxide support mol.
[c] Adsorbed volume under an equilibrium pressure of 66 Pa.

tively) with aqueous solutions containing known concentrations of the salts of the three additives. As salt precursors, lithium acetate (Strem), nickel formiate (J. Matthey), sulfuric acid (Prolabo, for the doped oxides) or ammonium sulfate (Prolabo, for the supported oxides), were chosen. Water was gently removed from the final solutions at 120°C. Eventually the dry solutions were calcined at 500°C for 3 h in air for the doped oxides, Li(Ni,S)-Al(Mg,Si)-1, and for 6 h in pure oxygen for the supported oxides, Li(Ni,S)-Al(Mg,Si)-10 and Li(Ni,S)-Al(Mg,Si)-50. The optimal temperature of calcination was chosen on the basis of the temperatures of decomposition of the precursor compounds resulting from thermal analysis experiments (TGA/DTA). The decomposition temperature of the precursors impregnated on the supports corresponded with those of the relevant compounds. The formation of Li_2O and NiO oxides on alumina and silica occurred at 400 and 300°C, respectively, and were associated with exothermic reactions. The decomposition of $(NH_4)_2SO_4$ was an endothermic reaction; on silica, before the complete decomposition to sulfate (confirmed by XPS analysis), the dimer compound $(NH_4)_3H(SO_4)_2$ was formed at 300°C. On magnesia support, a remarkable loss of mass was observed at 350°C due to $Mg(OH)_2$ decomposition. On this support, the decomposition of the cationic precursors was observed at 350°C [10,11], that of sulfate at 420°C [12], in agreement with literature. Therefore, calcination performed at 500°C ensured the complete decomposition of the three precursor compounds on the supports as well as that of surface $Mg(OH)_2$, preventing the evolution of Li_2O and the decomposition of sulfate.

2.2. Physico-chemical measurements

X-ray powder diffraction patterns (XRD) of the samples were collected on a computer-controlled Phillips diffractometer equipped with nickel-filtered Cu Kα radiation ($\lambda = 1.54178$ Å).

BET surface areas were determined from conventional N_2 adsorption isotherms. The samples were heated at 400°C for 2 h under vacuum (increasing rate of temperature = 2°C/min) before BET analysis.

Ammonia and sulfur dioxide were chosen as probe molecules to perform volumetric gas–solid titrations of the acid and basic sites of the samples. Ammonia and sulfur dioxide (Air Liquide, purity > 99.9%) were purified by successive freeze–thaw pumping cycles before use. Ammonia was previously dried on sodium wires.

The samples (~100 mg) were pretreated at 500°C with a 2°C/min increase rate under vacuum overnight before ammonia or sulfur dioxide adsorption. The adsorption temperature was maintained at 80°C in order to limit physisorption. The equilibrium pressure was measured by means of a differential pressure gauge (Datametrics).

2.3. Catalytic tests

The catalytic test of decomposition of isopropanol (IPA) was realized as described in refs. [3,6]. The reaction was carried out under inert atmosphere in a continuous-flow pyrex microreactor containing about 0.10 g of sample in powder form at atmospheric pressure. The feed was a mixture of isopropanol (purity grade > 99.9%) in nitrogen obtained by passing the nitrogen through the liquid isopropanol held in a saturator at 15°C. The gaseous mixture was further diluted with nitrogen to obtain partial pressures of isopropanol (P_{IPA}) in the range 600–2800 Pa. Typical runs were carried out with a total flow rate through the fixed bed of sample at 30 STP ml/min, with a P_{IPA} of 2800 Pa. Each run lasted at least 24 h. During the run, the reactor temperature was automatically changed in a random manner, to prevent a systematic influence of deactivation phenomena, in a range of about 80°C starting from the lower temperature at which some reactivity was detected. The reaction products, acetone (A), di-isopropyl ether (DIE), and propene (P) were automatically detected at 1 h intervals by an on-line gas chromatograph equipped with both FID and TCD detectors. A 2 m long stainless-steel column packed with Porapak Q was utilized; the column temperature was programmed from 55 to 140°C. By measuring the concentration of the isopropanol before and after the reactor as well as the concentration of the reaction products at the outlet of the reactor, conversion (X_{IPA} (%)) and selectivity to the three products (S_A (%), S_{DIE} (%) and S_P (%)) were calculated. Moreover, taking into account the contact time (0.2 g s ml^{-1}), the reaction rates to acetone (r_A), di-isopropyl ether (r_{DIE}), and propene (r_P) were calculated and expressed in μmol g^{-1} s^{-1}.

3. Results

3.1. Catalysts

The host oxides which were selected are commonly used as well as supports and catalysts. Considering that magnesia, alumina and silica take part in most of the acid–base reactions, to find a way to regulate or modify their surface properties appears as a fundamental objective. This can be effected either by adding very small amounts of metallic ions which will act as doping ions or by covering a larger surface of the support to give rise to supported oxides.

The selected additives (Li^+, Ni^{2+}, SO_4^{2-}) were chosen on the basis of their very different behaviors, as a basic alkali ion, a transition metal ion and an acidic sulfated ion. The ions were added on each support oxide in a concentration range between 0.1 and 16 μmol of metal ion per surface area which corresponds to a surface coverage of the support between 0.2 and 64% metal ion mol per

support oxide mol. Details on the composition of the samples and various surface coverages can be seen in table 1.

The interaction betweeen the support and the additives, in terms of anchorage points, determined the experimental surface coverage obtained. This can explain the failure in obtaining high degree of surface coverage in particular cases (i.e., S-Si-10, no anchorage point on silica surface, etc.).

The alumina series oxides did not display important modifications in the surface area values with reference to pure alumina, even when a high degree of surface coverage was realized (table 1). Starting from 208 m^2/g of pure alumina, among the aluminas modified with cationic additives, the lower surface values were those of Ni-Al-50 and Li-Al-50, with values of 180 and 190 m^2/g (decrease of 11%). When alumina was modified with sulfate, an increase of the surface was observed, in particular when high sulfate loading was realized (250 m^2/g for S-Al-50, increase of 18%). This can be due to the open structure of the sulfate groups deposited on the alumina surface. The analogous light influence of the additives on silica surface area values was observed (table 1). The values ranged from a minimum of 249 m^2/g for Li-Si-50 up to 335 m^2/g for Ni-Si-50, 18% and 8% of decrease and increase of areas, respectively, with respect to pure silica (310 m^2/g). Doping the magnesia surface with small amount of additives (1% of surface coverage), no important modification was created. Moreover, a deep decrease of the surface area values was observed with increasing lithium loading (i.e., Li-Al-10 and Li-Al-50). Due to the small ionic radius of Li^+ [13], it could hinder the microporosity of MgO leading to the observed loss of about 80% of the MgO surface. On magnesia too, the loading with high amount of sulfate (S-Mg-10 and S-Mg-50) caused enhanced values of surface areas.

All the modified oxides which have been studied remained amorphous (SiO_2) or crystalline (γ-Al_2O_3 and MgO periclase) phases of the relevant host oxides independent of the additive loading. In fact, XRD spectra of the samples did not reveal well detectable lines due to segregated oxide islands even for 50% of surface coverage. This could indicate that the guest oxides were well dispersed on the three host supports. One can also infer that the difficulty in detecting separate oxide phases was due to the difference between the mass of the guest (in particular for Li_2O and SO_3) and the host oxides (Al_2O_3, MgO, and SiO_2). Only for Ni-Al(Mg,Si)-50 samples, on which the deposition of a high amount of NiO (heavy atom) was performed, very light XRD lines typical of NiO phase were revealed. Therefore, it can be concluded that the doped as well as the supported oxides were prepared with acceptable good dispersion of the host oxides on the support surfaces.

As said above, the acid–base properties of the same samples have been determined by adsorption microcalorimetry using NH_3 and SO_2 as probe molecules. The volumetric and calorimetric results were already published [9] and table 1 gives only the respective volumes adsorbed under an equilibrium pressure of 66 Pa.

3.2. Catalytic test of isopropanol decomposition

The modification of the acid/base properties of the three oxide supports following the loading with Li^+, Ni^{2+}, and SO_4^{2-} ions were investigated by controlling the selectivity to the different products in the decomposition of isopropanol in inert atmosphere. As known from literature [8,14–16], the dehydration of alcohols on solid acids leads to olefin and ether, in particular propene and di-isopropyl ether, respectively, when considering IPA, whereas the dehydrogenation leads to ketones, in particular acetone when considering IPA. The nature of the solid acid and that of alcohol affect the reaction mechanism, as well as the oxidant or inert atmosphere and the reaction temperature can modify the selectivity to the main products [17,18]. The majority of primary and secondary alcohols react through an E_2 concerted mechanism, whereas tertiary alcohols react through a two-step E_1 mechanism, due to the higher stability of the intermediate carbocation. The E_1 mechanism requires only very strong acid sites, responsible for the formation of olefins, whereas the E_2 mechanism, involving both the acid and the basic sites of the solid, leads to ether formation, too [19]. In fact, literature reports that pure acidic solids, as silica–aluminas and zeolites [17] give more olefins than amphoteric oxides which have a balanced strength of acid and base sites, such as alumina. Alcohol dehydration can proceed also through the E_{1b} mechanism involving an intermediate carbanion on very basic solids which possess acid/base sites with imbalanced strength [20]. Concerning the dehydrogenation reaction, through an E_{1b} mechanism involving the same intermediate carbanion, the ketone is formed by an α-hydrogen abstraction [20–22]. The different reaction mechanisms which can occur on acid and basic solids for the IPA decomposition are diagrammed in fig. 1.

All the oxides studied have been tested in the reaction of IPA decomposition as a function of reaction temperature. The collected results in terms of kinetic parameters, calculated from the partial pressures of A, DIE, and P, are given in table 2. In this table, the temperature range in which the kinetic parameters were calculated is reported; the range corresponded to an IPA conversion $\leqslant 50\%$, even if a wider temperature interval was explored. The activation energy (E_a), the frequency factor (A), and the activation entropy values ($\Delta S^{\neq}$) have been calculated from the reaction rates obtained at different temperatures. They can be directly regarded as rate coefficients, since zero-order reactions for the formation of the three products were found at the P_{IPA} used in the kinetic runs for the whole temperature range covered [3], in accordance with literature, as well [15,21,23]. Therefore, by plotting $\ln(r_{A,DIE,P})$ vs. $1/T$, according

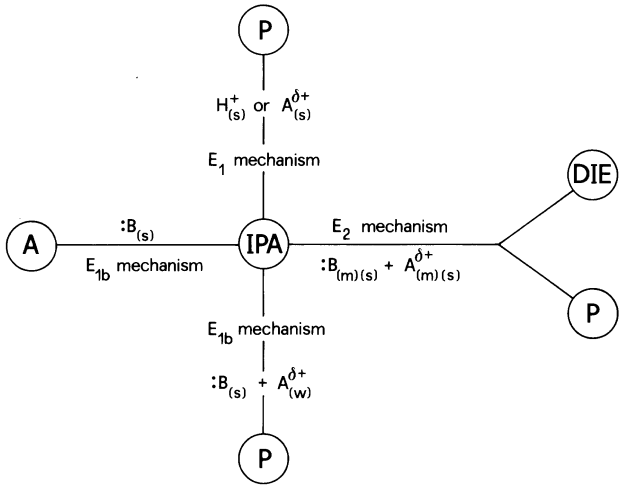

Fig. 1. Reaction mechanisms of IPA decomposition on acid and basic catalysts leading to dehydration products: DIE, di-isopropyl ether, and P, propene, and to dehydrogenation product: A, acetone. (H^+, Brønsted acid site; $A^{\delta+}$, Lewis acid site; :B, basic site; m, s, w indicate medium, strong, and weak sites.)

with the empirical Arrhenius law (eq. (1)), and $\ln(r_{A,DIE,P}/T)$ vs. $1/T$ according with the Eyring law (eq. (2)) for the transition state theory [24], the kinetic parameters for A, DIE, and P formation were obtained:

$$\ln r = \ln A - E_a/RT\,, \tag{1}$$

$$\ln(r/T) = \ln(k_B/h) + \Delta S^{\neq}/R - \Delta E/RT + \ln C_a - (\Delta n^{\neq} - 1)\,, \tag{2}$$

where k_B and h are Boltzmann's and Planck's constants, respectively, R is the gas constant, ΔE is the activation energy, C_a is the surface concentration of the reactant (IPA) in a complete monolayer (in accordance with a zero-order reaction), and $\Delta n^{\neq}$ is the change in number of molecules during the formation of the transition state. C_a was calculated according to ref. [25] from the liquid density of IPA. The entropy at a surface concentration of 1 mol/g was taken as standard state. As reported in ref. [3] and according to other authors [19,26], $\Delta n^{\neq} = 0$ for acetone and propene formation and $\Delta n^{\neq} = -1$ for di-isopropyl ether formation were considered in the computation. In order to give an indication of the accuracy of the parameters, the estimated standard errors of the calculated parameters are reported in table 2.

3.2.1. Alumina series oxides

Pure alumina oxide displayed catalytic activity starting from 160°C, the Li^+ addition caused a decrease in the ability of IPA decomposition, the temperature at which 10% of IPA conversion was observed increased from 167°C, for Al_2O_3, to 173, 215, and 280°C for Li-Al-1, Li-Al-10, and Li-Al-50, respectively. This behavior could indicate a decrease of surface acidity. The addition of sulfate on Al_2O_3 caused an opposite trend: a decrease of the temperature at which 10% of IPA conversion was observed, increasing the sulfate loading (166, 148, and 136°C for S-Al-1, S-Al-10, and S-Al-50, respectively). This behavior reflects an increase of the surface acidity. In the case of lithium and sulfate additives, propene and di-isopropyl ether were the only products formed. The loading with nickel modified the alumina surface in a more complicated way, a progressive decrease of DIE and P formation was oberved going from Ni-Al-1 to Ni-Al-50. On this latter sample acetone formation was observed. To facilitate the comparison among the catalyst activities of the different alumina series oxides, the rates for A, DIE, and P formation were reported at the temperature of 180°C (fig. 2). The reaction rates were calculated either by interpolation or extrapolation using the Arrhenius parameters of table 2. The extrapolations were justified by the good linearity of the experimental points. Due to the amphoteric properties of the alumina surfaces having acid/base sites of balanced strength [3,27,28], the E_2 mechanism can be claimed for the formation of the dehydration products, DIE and P [17]. The presence of a high amount of nickel on the Al_2O_3 surface, Ni-Al-50, changed completely the reaction mechanism of IPA decomposition. The surface lost almost completely its dehydration ability. Accordingly, our experimental volumetric results showed that Ni-Al-50 has a lack of acid/base sites of balanced strength. In this case, the occurrence of a small amount of acetone could be justified by the dehydrogenation ability of nickel cation rather than an increase of basicity of the surface, as indicated from volumetric results of SO_2 adsorption (see table 1).

3.2.2. Magnesia series oxides

Since magnesia surfaces displayed poor dehydrogenation and dehydration activity, a temperature range as high as 200–300°C had to be utilized to detect the reaction products. In this temperature range, IPA conversion was lower than 20%, except for Li(Ni,S)-Mg-10. These samples attained, at the highest tested temperatures (280–300°C), 40–60% of X_{IPA}. Interesting modifications were observed in the selectivity to the three main products following the loading with the three additives. Propene was the main product in every case. The presence of lithium on MgO did not alter the catalytic properties of the magnesia surface. Even if more basic surfaces were created with respect to MgO (see table 1), acetone was never observed among the reaction products. Depending on Li^+ loading, the ratio between the two main products, DIE and P, changed. A remarkable increase of propene formation was noticed on Li-Mg-10. The loading with nickel deeply modified the magnesia surface starting from the doped oxide, Ni-Mg-1. The mechanism of IPA decomposition changed, as can be observed from the appearance of acetone among the reaction products. Concerning the effect of sulfate, no important modification in terms of selectivity or total

Table 2
Kinetic parameters for the catalytic decomposition of isopropanol of the loaded oxides and corresponding supports

Sample	Temperature range (°C)	E_a (kJ/mol)			ln A (A/mol g^{-1} s^{-1})			$\Delta S^{\neq}$ (J/(mol K))		
		A [a]	DIE [b]	P [c]	A [a]	DIE [b]	P [c]	A [a]	DIE [b]	P [c]
Al	160–185	–	91.92 ± 5	122.72 ± 2	–	8.385 ± 1.4	18.860 ± 0.44	–	−147.97 ± 12	−52.59 ± 4
Li-Al-1	160–195	–	102.66 ± 8	125.86 ± 4	–	10.218 ± 2.1	18.687 ± 1.04	–	−132.85 ± 17	−54.12 ± 9
Li-Al-10	180–206	–	137.69 ± 4	143.87 ± 2	–	17.129 ± 1.1	21.221 ± 0.60	–	−75.80 ± 9	−33.43 ± 5
Li-Al-50	180–280	–	–	124.47 ± 2	–	–	12.150 ± 0.43	–	–	−109.24 ± 4
Ni-Al-1	165–200	–	75.31 ± 9	106.83 ± 6	–	3.797 ± 2.4	14.369 ± 1.5	–	−186.04 ± 20	−89.85 ± 13
Ni-Al-10	137–190	–	112.53 ± 12	133.80 ± 6	–	12.513 ± 2.4	20.955 ± 1.7	–	−113.43 ± 20	−34.67 ± 14
Ni-Al-50	180–230	68.37 ± 8	96.61 ± 8	131.08 ± 4	−1.019 ± 1.9	6.696 ± 2.0	18.000 ± 1.0	−217.21 ± 16	−161.38 ± 17	−59.08 ± 8
S-Al-1	160–200	–	61.91 ± 12	109.06 ± 4	–	0.150 ± 3.3	14.795 ± 1.0	–	−216.24 ± 27	−86.17 ± 8
S-Al-10	140–200	–	106.80 ± 9	138.10 ± 12	–	12.398 ± 2.4	23.095 ± 3.2	–	−114.86 ± 20	−17.16 ± 26
S-Al-50	120–150	–	81.13 ± 7	127.93 ± 5	–	6.847 ± 2.1	22.352 ± 1.3	–	−161.56 ± 17	−24.34 ± 11
Mg	230–320	–	72.30 ± 4	122.72 ± 4	–	−2.625 ± 0.9	12.823 ± 7.2	–	−235.92 ± 7	−99.10 ± 7
Li-Mg-1	230–285	–	–	129.70 ± 7	–	–	13.296 ± 1.5	–	–	−95.99 ± 12
Li-Mg-10	200–260	–	103.85 ± 5	124.74 ± 5	–	7.231 ± 1.1	15.650 ± 1.3	–	−137.20 ± 9	−58.96 ± 10
Li-Mg-50	200–250	–	105.58 ± 3	153.49 ± 3	–	4.692 ± 0.8	20.077 ± 0.7	–	−157.32 ± 6	−20.94 ± 6
Ni-Mg-1	210–260	53.24 ± 4	–	140.51 ± 7	−2.649 ± 0.9	–	16.214 ± 1.5	−227.48 ± 8	–	−70.66 ± 13
Ni-Mg-10	250–300	11.49 ± 3	34.57 ± 11	66.20 ± 6	7.651 ± 0.7	−9.816 ± 2.5	1.522 ± 1.3	−143.65 ± 6	−296.86 ± 21	−194.56 ± 11
Ni-Mg-50	190–260	61.18 ± 8	–	160.30 ± 6	−1.498 ± 2.0	–	20.978 ± 1.3	−218.08 ± 17	–	−31.36 ± 11
S-Mg-1	230–270	–	97.00 ± 8	131.39 ± 4	–	2.432 ± 1.7	14.772 ± 0.9	–	−194.37 ± 14	−83.31 ± 8
S-Mg-10	230–290	–	75.16 ± 8	96.90 ± 3	–	−1.152 ± 1.7	8.108 ± 0.6	–	−225.29 ± 15	−140.12 ± 5
S-Mg-50	200–220	–	–	157.82 ± 6	–	–	21.456 ± 1.4	–	–	−30.00 ± 11
Si	220–250	–	–	144.07 ± 5	–	–	17.773 ± 1.1	–	–	−65.95 ± 9
Li-Si-1	230–305	–	52.93 ± 13	101.86 ± 3	–	−6.869 ± 2.9	8.197 ± 0.7	–	−278.99 ± 24	−145.42 ± 6
Li-Si-10	200–260	–	56.41 ± 8	71.74 ± 13	–	−5.268 ± 1.9	2.631 ± 3.0	–	−264.92 ± 15	−190.93 ± 25
Li-Si-50	200–230	–	–	156.89 ± 6	–	–	22.013 ± 1.5	–	–	−28.58 ± 12
Ni-Si-1	215–250	–	–	149.25 ± 9	–	–	20.309 ± 2.2	–	–	−44.77 ± 18
Ni-Si-10	200–260	83.54 ± 5	79.86 ± 12	123.12 ± 7	5.171 ± 1.1	2.156 ± 2.8	15.817 ± 1.6	−169.82 ± 9	−203.21 ± 23	−81.32 ± 13
Ni-Si-50	200–230	104.76 ± 7	–	–	10.226 ± 1.7	–	–	−129.01 ± 14	–	–
S-Si-1	225–300	–	–	122.22 ± 2	–	–	12.042 ± 0.4	–	–	−113.08 ± 3
S-Si-10	150–200	–	39.62 ± 7	97.18 ± 5	–	−7.564 ± 1.9	11.605 ± 1.2	–	−283.16 ± 16	−115.47 ± 10

Reaction products: [a] A, acetone; [b] DIE, di-isopropyl ether; [c] P, propene.

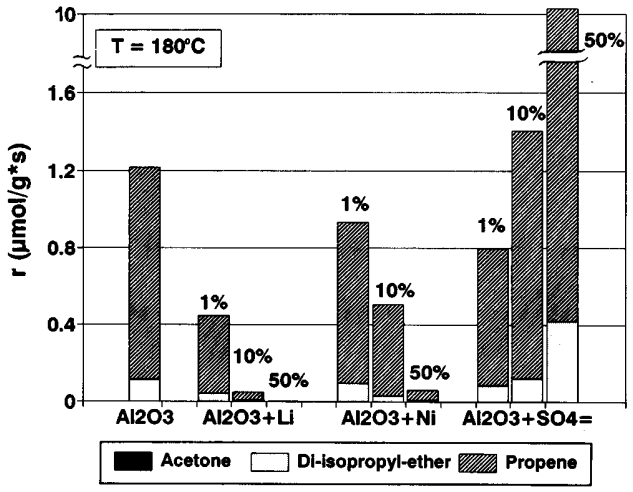

Fig. 2. Comparison of acetone, di-isopropyl ether, and propene formation from IPA decomposition at 180°C, in terms of intrinsic rates for the alumina series oxides at various surface coverages of additive.

IPA conversion was observed. Fig. 3 displays, for the MgO surfaces, the rates of A, DIE, and P formation calculated by using the Arrhenius parameters reported in table 2, compared at 220°C. This temperature corresponded to $X_{IPA} < 10\%$ in every case. The more characteristic feature shown by this series of oxide surfaces was the remarkable increase of propene formation on the supported samples, Li(Ni,S)-Mg-10, and the abrupt decrease on high-loaded supported oxides, Li(Ni,S)-Mg-50. This behavior can be related to modification of the acid/base population sites following the increase of the additive loading. The MgO surfaces possess very strong basicity, in terms of both number and strength of their basic sites, although some acid sites are present [3,4,27]. This picture could justify the formation of propene through the E_{1b} mechanism requiring acid–base pairs of imbalanced strength (strong basic sites). The sample Li-Mg-10, on which high amount of propene was formed, has surface basic sites of high strength [9] (average heat of SO_2 adsorption, $Q_{av(SO_2)} = 104$ kJ/mol), together with an appreciable number of acid sites of very low acid strength [9] (average heat of NH_3 adsorption, $Q_{av(NH_3)} = 4.4$ kJ/mol). Li-Mg-50, however, has very basic surface and no acidity. This could justify the poor propene formation.

3.2.3. Silica series oxides

The silica series oxides displayed catalytic activity in the same temperature range as the magnesia surfaces. The loading of the three additives on silica surface starting from a loading of about 10% of surface coverage, Li(Ni,S)-Si-10(50), changed significantly the activity of SiO_2, as shown in fig. 4. The comparison in terms of reaction rates, r_A, r_{DIE}, and r_P calculated from the Arrhenius parameters of table 2, has been made at reaction temperature of 220°C. At this temperature, X_{IPA} ranged from 2 to 10%, except for Ni(S)-Si-10 which attained about 50% of X_{IPA}. Pure SiO_2 formed only little amount of propene, the basic sites being too weak to give rise to ether formation. The addition of Li^+ gave rise to higher IPA conversion and selectivity to DIE was observed too. This reflects the increase of basicity of the surfaces modified with Li^+ (table 1) which could decompose isopropanol through an E_2 mechanism. The presence of nickel on the silica surface completely changed the IPA decomposition activity of SiO_2. Ni-Si-10 formed acetone and both di-isopropyl ether and propene as dehydration products, Ni-Si-50 had only dehydrogenation ability giving acetone as unique reaction product. The addition of sulfate in an ionic concentration as low as 0.08 μmol/m^2 (S-Si-1) did not cause detectable modification of the silica sur-

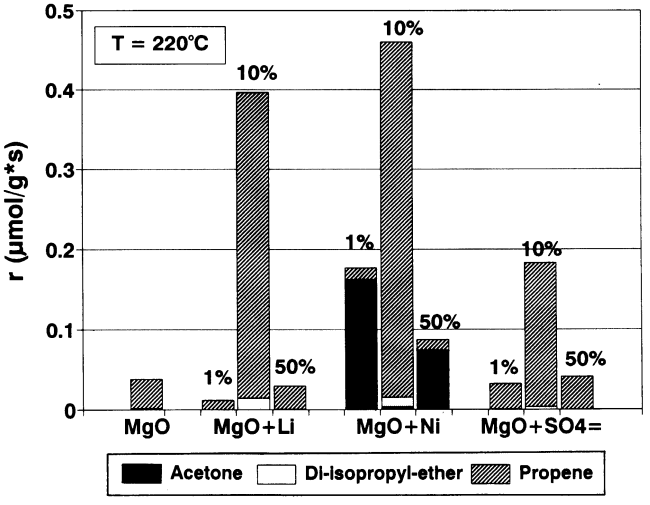

Fig. 3. Comparison of acetone, di-isopropyl ether, and propene formation from IPA decomposition at 220°C, in terms of intrinsic rates for the magnesia series oxides at various surface coverages of additive.

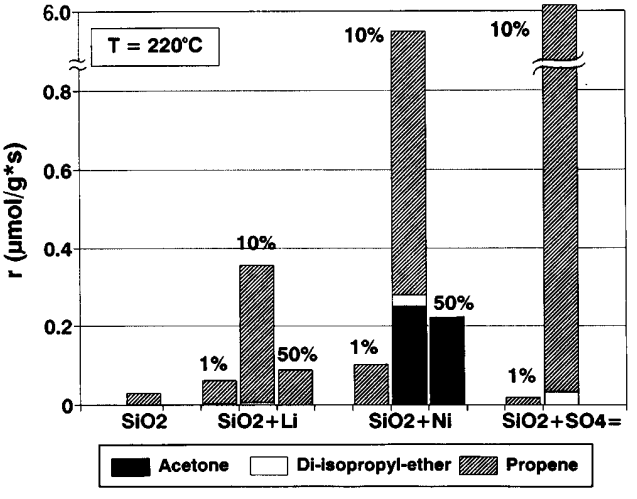

Fig. 4. Comparison of acetone, di-isopropyl ether, and propene formation from IPA decomposition at 220°C, in terms of intrinsic rates for the silica series oxides at various surface coverages of additive.

face as concerns the catalytic activity. By contrast, the presence of sulfate in higher amount, 0.17 μmol/m^2 (S-Si-10) led to remarkable increase of IPA conversion and formation of appreciable amount of di-isopropyl ether. The weak amphoteric character of silica was strengthened by sulfate addition.

4. Discussion

The understanding of the acid/base properties of the modified surfaces studied can be approached on the basis of the calculated kinetic parameters of the test reaction of isopropanol decomposition. With this perspective, we consider that the number and the nature of the sites should mainly affect the Arrhenius parameters, A, the strength of the sites should mainly affect the activation energy [3,6], E_a, and the reaction path (formation of "activated complex") should be reflected by the activation entropy, $\Delta S^{\neq}$ [3]. Therefore, the kinetic parameters collected in table 2 can be related to the acidity/basicity of the oxide surfaces, in a complementary way with the volumetric–calorimetric results.

As expected, the values of E_a for the formation of propene ($E_{a\,P}$) were, as a general trend, higher than those of di-isopropyl ether ($E_{a\,DIE}$) and acetone ($E_{a\,A}$) formation. The $E_{a\,P}$ value for Al_2O_3 was 123 kJ/mol, the values for the modified alumina oxides were in a narrow range (107–144 kJ/mol). $E_{a\,P}$ values for magnesia series oxides were widened, going from a minimum of 66 and 97 kJ/mol, for Ni-Mg-10 and S-Mg-10 up to 160 kJ/mol for Ni-Mg-50. In this case, it is not possible to obtain valuable information on the acidity/basicity of the surfaces. It is known that basic and amphoteric oxides having strong basic and weak acidic surface sites can form either acetone or propene depending on the temperature and on experimental conditions (i.e., oxidant or inert atmosphere). For this reason, the decomposition of alcohol cannot be utilized as good test to study the character of sites of basic solids. The $E_{a\,P}$ values for the modified silica surfaces were lower than that of pure silica in agreement with a strengthening of the acidity and amphoteric properties of the loaded oxides. More appreciable differences among the $E_{a\,DIE}$ values were found for the three series of oxides. The lesser the $E_{a\,DIE}$ values (i.e., Ni-Al-1, S-Al-1, Ni-Mg-10, Li-Si-1(10)), the higher the amphoteric character of the surfaces in terms of balanced strength of the acid/base sites.

As regards the Arrhenius parameter A, no appreciable differences were noticed among the frequency factors for P formation ($\ln A_P$, as reported in table 2) on alumina series oxides. Only Li-Al-50 has $\ln A_P$ value much lower ($\ln A_P = 12.15$) than those of the other alumina samples (average value $\ln A_P = 19.15$). This sample, as reported in table 1, has a high number of basic sites and low number of acid sites; this situation might justify a catalytic behavior different from that of pure alumina and the other modified alumina surfaces. The $\ln A_P$ for the magnesia surfaces were in a wide range (8.1–21.5) reflecting deep variation of the number and nature of the acid and basic sites of these surfaces. Regarding the SiO_2 series oxides, it can be noticed that when the modified surfaces were able to form di-isopropyl ether, the $\ln A_P$ values were low (average value $\ln A_P = 7$), while when only propene were formed, the values were higher (average value $\ln A_P = 18$). This could be diagnostic of changes in the nature of the acid/base sites of the surfaces. For the three series of oxide samples, the values of $\ln A_{DIE}$ were more affected by the loading of the surfaces than the relevant $\ln A_P$ values. It is really difficult to find a group of samples having similar $\ln A_{DIE}$ values. As discussed above, for ether formation both an acid site and a base site is necessary, and since the nature of both the sites is expected to affect the frequency factor value, this complicates the interpretation of the $\ln A_{DIE}$ values.

The physical meaning of the activation entropies, $\Delta S^{\neq}$, according with theory of absolute reaction rates following a "thermodynamic approach", is connected to the possibility of estimating the properties of the activated complex [24]. If $\Delta S^{\neq}$ is positive, corresponding to a more probable activated complex, the reaction is faster than normal. On the contrary, if $\Delta S^{\neq}$ is negative, the activated complex is less probable and the rate slower. In any event, $\Delta S^{\neq}$ is expected to become more negative for a reaction between two polyatomic molecules than for a reaction between two atoms or involving only one polyatomic molecule. An inspection of the calculated $\Delta S^{\neq}$ values from the experimental rates of A, DIE, and P formation (table 2) reveals that, as a general trend, more highly negative entropies of activation were found for acetone and di-isopropyl ether formation than those for propene formation [3]. The highly negative $\Delta S^{\neq}$ values for DIE are expected as the entropy loss in the formation of the transition state is higher when two molecules are adsorbed on the surface than when only one molecule is involved, as above discussed. Regarding the $\Delta S^{\neq}$ values for A formation compared with those for P formation, the highly negative values for the former ones reflect a high loss of vibrational degree of freedom of IPA reactant molecule in the transition state. Two different sets of $\Delta S^{\neq}$ values for P formation have been found, the more negative values are in the range -122 ± 38 J/(mol K) and the less negative in the range -43 ± 21 J/(mol K). Assuming the localized adsorbed reactant to be the initial state and neglecting rotational contributions, the two different sets of $\Delta S^{\neq}$ values may be explained, to a first approximation, by differences of the vibrational partition functions in the ground and transition states of the reactant molecule, IPA. The higher the E_1 character the more pronounced is the Cα–O bond fission of IPA molecule (ionic character) which results in a higher loss of vibrational degree of freedom and therefore leads to a highly negative entropy of activation. The E_2-like reac-

tion intermediate exhibits also a certain ionic character [18,26]. However, with increasing the E_2 character, the Cα–O bond loosening of IPA molecule is weaker, the double bond is preformed, and the β-hydrogen forms a bond to the basic site. Therefore, some bonds are weakened and the respective force constants are lowered; however, other bonds are strengthened and new bonds are formed. Completely different sets of force constants and frequencies between the E_1 and E_2 reaction intermediates have to be considered for the ground and transition states. Eventually, it can be inferred that the higher the E_2 character of the transition state, the lower is the entropy loss in the formation of the transition state. Following this argument, the more negative $\Delta S^{\neq}$ values could be associated with E_2-like reaction intermediates with higher ionic character. In terms of acidity/basicity of the surfaces this signifies the presence of amphoteric surface with acid/base sites of not balanced strength. All the alumina series oxides, except Li-Al-50, have moderate negative $\Delta S^{\neq}$ values (average value 50 J/(mol K)). Magnesia and silica series oxides have a more heterogeneous behavior in terms of the $\Delta S^{\neq}$ values, reflecting important differences in the nature and strength of their surface acid/base sites. In particular when very high $\Delta S^{\neq}$ values were observed (i.e., Ni-Mg-10 and Li-Si-10), a more ionic reaction intermediate could be inferred, as the E_{1b}-like intermediate is due to the strong basicity of the surfaces.

Fig. 5 represents the rates of propene formation on the modified alumina samples measured at 180°C as a function of the number of total acidic sites determined by ammonia adsorption for an equilibrium pressure of 66 Pa. There is a pretty good correlation between these two approaches of the acidity measurement and the dotted lines of the figure confirm that the addition of sulfate increases both the acidity and catalytic activity while the addition of nickel or lithium decreases both.

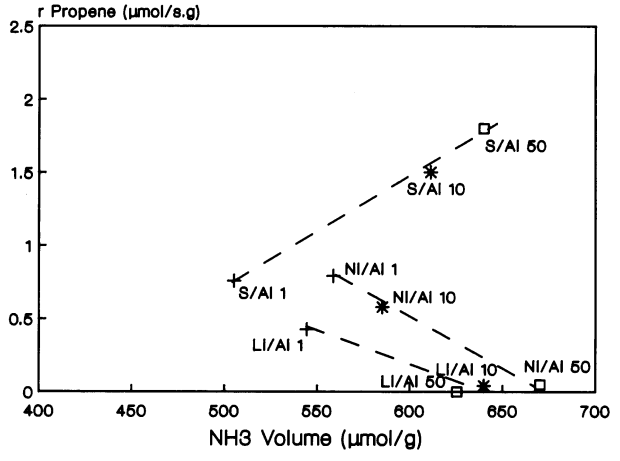

Fig. 5. Rate of propene formation at 180°C as a function of the number of acidic sites from ammonia adsorption (adsorbed volume at 66 Pa).

5. Conclusion

Modification of alumina, silica or magnesia with small amounts of other oxides has a considerable influence on their acid/base properties. The change in these properties depends on the nature and amount of the modifying oxide introduced, as shown by the reaction of isopropanol decomposition.

Important perturbations of the surfaces are reflected by the change of the reaction products, while the kinetic parameters of the reaction are more related to perturbations of the significant fraction of sites which are involved in the reaction mechanism. Acidic and amphoteric surfaces can be more directly diagnosed by the test reaction of IPA decomposition, in the present situation alumina and silica series oxides, while the results obtained on basic surfaces, in the present case magnesia series oxides, have to be evaluated with more care [6]. Moreover, the approach has to be made with homogeneous series of catalysts in terms of nature and strength of the active acid/base sites, otherwise wide heterogeneity of catalysts can prevent simple relationships from being diagnosed. This conclusion was supported by our experimental data on the three distinct series of alumina, magnesia, and silica surfaces.

References

[1] K. Tanabe, in: *Catalysis, Science and Technology*, Vol. 8, eds. J.R. Anderson and M. Boudart (Springer, Berlin, 1987) pp. 232–271.
[2] Y. Chen and L. Zhang, Catal. Lett. 12 (1992) 51.
[3] A. Gervasini, G. Bellussi, J. Fenyvesi and A. Auroux, J. Phys. Chem. 99 (1995) 5117.
[4] A. Gervasini, G. Bellussi, J. Fenyvesi and A. Auroux, in: *New Frontiers in Catalysis*, Proc. 10th Int. Congr. on Catalysis, eds. L. Guczi, F. Solymosi and P. Tétényi (Elsevier, Amsterdam, 1993) pp. 2047–2050.
[5] N.A. Youssef and A.M. Youssef, Bull. Soc. Chim. Fr. 128 (1991) 864.
[6] A. Gervasini and A. Auroux, J. Catal. 131 (1991) 190.
[7] M. Ai, J. Catal. 52 (1978) 16.
[8] K. Tanabe, M. Misono, Y. Ono and H. Hattori, in: *New Solid Acids and Bases, Their Catalytic Properties*, Vol. 51, eds. B. Delmon and J.T. Yates (Elsevier, Amsterdam, 1989).
[9] A. Gervasini, J. Fenyvesi and A. Auroux, Langmuir (1996), to be published.
[10] K. Jiràtovà and L. Beránek, Appl. Catal. 2 (1982) 125.
[11] V. Perrichon and M.C. Durupty, Appl. Catal. 42 (1988) 217.
[12] A. Amin, S. Hanafi and S.A. Selim, Thermochim. Acta 53 (1982) 125.
[13] R.D. Shannon, Acta Cryst. 32 (1976) 751.
[14] J. Cunningham, B.K. Hodnett, M. Ilyas, E.L. Leahy and J.L.G. Fierro, Faraday Discussions Chem. Soc. 72 (1981) 283.
[15] M. Ai, Bull. Chem. Soc. Jpn. 50 (1977) 2579.
[16] H. Nollery and G. Ritter, J. Chem. Soc. Faraday Trans. I 80 (1984) 275.
[17] J.C. Luy and J.M. Parera, Appl. Catal. 26 (1986) 295.
[18] H. Knözinger and A. Scheglila, J. Catal. 17 (1970) 252.
[19] V.R. Padmanabhan and F.J. Eastburn, J. Catal. 24 (1972) 88.
[20] I. Halasz, H. Vinek, K. Thomke and H. Noller, Z. Phys. Chem. NF 144 (1985) 157, and references therein.

[21] E. Akiba, M. Soma, T. Onishi and K. Tamaru, Z. Phys. Chem. 119 (1980) 103.
[22] K.C. Waugh, M. Bowker, R.W. Petts, H.D. Vandervell and J. O'Malley, Appl. Catal. 25 (1986) 121.
[23] H. Knözinger, H. Buhl and E. Ress, J. Catal. 12 (1968) 121.
[24] J.W. Moore and R. Pearson, in: *Kinetics and Mechanism* (Wiley, New York, 1981) pp. 177–181.
[25] P.H. Emmett and S. Brunauer, J. Am. Chem. Soc. 59 (1937) 1553.
[26] H. Knözinger, H. Buhl and K. Kochloefl, J. Catal. 24 (1972) 57.
[27] A. Auroux and A. Gervasini, J. Phys. Chem. 94 (1990) 6371.
[28] A. Gervasini and A. Auroux, J. Phys. Chem. 97 (1993) 2628.